The Sac1 Domain of SYNJ1 Identified Mutated in a Family with Early-Onset Progressive Parkinsonism with Generalized Seizures

13 AUTHORS, INCLUDING:

Catharine E. Krebs
University of California, Los Angeles
7 PUBLICATIONS **74** CITATIONS

SEE PROFILE

Siamak Karkheiran
12 PUBLICATIONS **73** CITATIONS

SEE PROFILE

Gilbert Di Paolo
Columbia University
80 PUBLICATIONS **6,890** CITATIONS

SEE PROFILE

Zhenyu Yue
Icahn School of Medicine at Mount Sinai
51 PUBLICATIONS **6,619** CITATIONS

SEE PROFILE

RAPID COMMUNICATION

Human Mutation

OFFICIAL JOURNAL

HGVS
HUMAN GENOME
VARIATION SOCIETY
www.hgvs.org

The Sac1 Domain of *SYNJ1* Identified Mutated in a Family with Early-Onset Progressive Parkinsonism with Generalized Seizures

Catharine E. Krebs,[1][†] Siamak Karkheiran,[2][†] James C. Powell,[1] Mian Cao,[3] Vladimir Makarov,[4] Hossein Darvish,[5] Gilbert Di Paolo,[6] Ruth H. Walker,[1,7] Gholam Ali Shahidi,[8] Joseph D. Buxbaum,[9–14] Pietro De Camilli,[3] Zhenyu Yue,[1,11,14] and Coro Paisán-Ruiz[1,10,12–14]*

[1]Department of Neurology, Icahn School of Medicine at Mount Sinai, New York City, New York; [2]Movement Disorders Clinic, Hazrat Rasool Hospital, Tehran University of Medical Sciences, Tehran, Iran; [3]Howard Hughes Medical Institute, Department of Cell Biology and Program in Cellular Neuroscience, Neurodegeneration and Repair, Yale University School of Medicine, New Haven, Connecticut; [4]Department of Biostatistics, Mailman School of Public Health, Columbia University, New York City, New York; [5]Department of Medical Genetics, Shahid Beheshti University of Medical Sciences, Tehran, Iran; [6]Department of Pathology and Cell Biology, Taub Institute for Research on Alzheimer's Disease and the Aging Brain, Columbia University Medical Center, New York City, New York; [7]Department of Neurology, James J. Peters Veterans Affairs Medical Center, Bronx, New York; [8]Department of Neurology, Hazrat Rasool Hospital, Tehran University of Medical Sciences, Tehran, Iran; [9]Seaver Autism Center for Research and Treatment, Mount Sinai School of Medicine, New York City, New York; [10]Department of Psychiatry, Icahn School of Medicine at Mount Sinai, New York City, New York; [11]Department of Neurosciences, Icahn School of Medicine at Mount Sinai, New York City, New York; [12]Department of Genetics and Genomic sciences, Icahn School of Medicine at Mount Sinai, New York City, New York; [13]Mindich Child Health and Development Institute, Icahn School of Medicine at Mount Sinai, New York City, New York; [14]Friedman Brain Institute, Icahn School of Medicine at Mount Sinai, New York City, New York

ABSTRACT: This study aimed to elucidate the genetic causes underlying early-onset Parkinsonism (EOP) in a consanguineous Iranian family. To attain this, homozygosity mapping and whole-exome sequencing were performed. As a result, a homozygous mutation (c.773G>A; p.Arg258Gln) lying within the NH_2-terminal Sac1-like inositol phosphatase domain of polyphosphoinositide phosphatase synaptojanin 1 (SYNJ1), which has been implicated in the regulation of endocytic traffic at synapses, was identified as the disease-segregating mutation. This mutation impaired the phosphatase activity of SYNJ1 against its Sac1 domain substrates in vitro. We concluded that the *SYNJ1* mutation identified here is responsible for the EOP phenotype seen in our patients probably due to deficiencies in its phosphatase activity and consequent impairment of its synaptic functions. Our finding not only opens new avenues of investigation in the synaptic dysfunction mechanisms associated with Parkinsonism, but also suggests phosphoinositide metabolism as a novel therapeutic target for Parkinsonism.

Introduction

Early-onset Parkinsonism (EOP) is characterized by the presentation at a young age of tremor, hypokinesia, muscular rigidity, and postural instability [Jankovic, 2008]. Parkinsonism may have many etiologies, including metabolic or infectious diseases, pharmacotherapy, or genetic causes. During the past years, a number of inherited forms, which are usually characterized by juvenile onset, L-dopa responsiveness, and recessive pattern of inheritance, have been described [Martin et al., 2011; Paisan-Ruiz et al., 2010]. To date, there are at least six different genes associated with autosomal recessive EOP (AR-EOP): PARK2 (*PRKN*; MIM #600116), PARK6 (*PINK1*; MIM #605909), PARK7 (*DJ-1*; MIM #602533), PARK9 (*ATP13A2*; MIM #606693), PARK14 (*PLA2G6*; MIM #612953), and PARK15 (*FBXO7*; MIM #260300) [Hardy et al., 2009]. Mutations in *PRKN*, *PINK1*, and *DJ-1* cause more typical Parkinsonism while *ATP13A2*, *PLA2G6*, and *FBXO7* mutations are responsible for complex syndromes, with pyramidal signs, cognitive decline, as well as other neurological and psychiatric symptoms, and may become nonresponsive to levodopa treatment with the disease progression [Paisan-Ruiz et al., 2010]. Additionally, *PRKRA* (DYT16; MIM #612067) and Spactasin (SPG11; MIM #610844) mutations have also been reported in juvenile atypical Parkinsonism forms and *SLC6A3* mutations are known to cause infantile

dystonia-Parkinsonism syndrome (PKDYS; MIM #613135) [Camargos et al., 2008; Kurian et al., 2009; Paisan-Ruiz et al., 2010]. More recently, mutations within *DNAJC6* (MIM #608375) encoding auxilin, a protein implicated in clathrin-mediated endocytosis, have been identified in families featuring autosomal recessive juvenile Parkinsonism [Edvardson et al., 2012; Koroglu et al., 2013].

In the current study, we aimed to identify the genetic causes underlying disease in a consanguineous family of Iranian ancestry featuring EOP with generalized seizures. Whole-exome sequencing (WES), particularly in conjunction with other methods like SNPs-based arrays, has become a fruitful strategy for gene identification in both complex and Mendelian traits and as such is an ideal approach to identify disease causal alleles [Krebs and Paisan-Ruiz, 2012; Singleton, 2011]. Therefore, homozygosity mapping (HM) through high-throughput SNP genotyping followed by WES and disease-segregation analyses was performed for disease-locus and gene identification. As a result, we identified a disease-segregating mutation, c.773G>A causing p.Arg258Gln, within the NH$_2$-terminal SAC1-like inositol phosphatase (Sac1) domain of the polyphospho-inositide phoshatase SYNJ1 (MIM #604297), which also contains an inositol 5-phosphatase domain and a COOH-terminal proline-rich region that interacts with a variety of SH3 domain-containing endocytic factors, such as endophilin and amphiphysin [Dittman and Ryan, 2009]. We later evaluated the effects of the p.Arg258Gln mutation on the enzymatic properties of SYNJ1 and concluded that the *SYNJ1* p.Arg258Gln mutation impairs the Sac1-like phosphatase activity. Our current finding not only opens a new avenue of investigation in the field of Parkinson research, but also adds new evidence that defects in membrane traffic at the synapse may be key factors in the development of both Parkinson disease and Parkinsonism.

Methods

Subjects

A consanguineous family featuring EOP was clinically examined. The family consisted of healthy parents, who were first-degree relatives, two affected, and three unaffected siblings (Figure 1). The local ethics committee at Tehran University of Medical Sciences approved this study and informed consent was obtained from all participants. DNA samples from all members were isolated from whole blood using standard procedures.

Genetic variants identified within disease-associated loci (Tables 1 and 2) were additionally tested by direct Sanger sequencing in 96 DNA samples belonging to controls individuals of Iranian ancestry from the same geographical region of our family and 92 DNA samples of Caucasian neurologically normal individuals available to purchase at Coriell Cell Repository (NDPT093; http://www.coriell.org/).

Twenty DNA samples of affected individuals with EOP were also tested for the entire coding region of *SYNJ1*. Although seizures were not present in any of these patients, all presented with complex EOP, including Parkinsonism, spasticity, and dystonia as common phenotypic features.

Genome-Wide SNP Genotyping and Homozygosity Mapping

SNP genotyping was performed in all available family members (*n* = 7) using the HumanOmniExpress beadchips and HiScanSQ system (Illumina Inc., San Diego, CA). Genotyping quality assessments were undertaken according to the appropriate options within the Genome Studio program (GS; Illumina). PLINK input reports

were generated within the GS and uploaded to PLINK v1.07 program [Purcell et al., 2007]. Homozygous segments were identified using the ROH tool (Runs of homozygosity) within PLINK, where a minimum physical size threshold of 1 Mb and at least 100 homozygous adjacent markers in length, including no more than two SNPs with missing genotypes and only one possible heterozygous genotype, were used as inclusion criteria. Subsequently, overlapping and potentially matching segments were also identified in PLINK using an allelic matching of 0.99 as threshold. Homozygous segments were also visualized using the Illumina genome viewer within the GS program.

Whole-Exome Sequencing

WES was performed in both affected siblings. The SureSelect Human All exon 50 Mb exon-capture kit was used for library enrichment (Agilent Technologies Inc., Santa Clara, CA). The captured exome libraries were then sequenced on a HiSeq2000 according to the manufacturer's instructions for paired-end 100-bp reads (Illumina Inc.) and on a single flow cell lane. After sequencing, data were put through a computational pipeline for WES data processing and analysis following the general workflow adopted by the 1000 genomes project [DePristo et al., 2011]. First, the alignment of raw sequence reads to the human reference genome sequence (NCBI GRCh37) was performed using a fast lightweight Burrows–Wheeler Alignment Tool [Li and Durbin, 2009]. The Genome Analysis Toolkit (GATK v1.5–16-g58245bf) was then used for base-quality recalibration and local realignment to minimize base calling error and mapping error, respectively. Lastly, the GATK Unified Genotyper tool was employed to call single-nucleotide substitutions (SNP/SNV) and short insertions/deletions (INDEL). Only passing variants were included in the final variant set. Calls were filtered based on the mapping quality (q30 or higher) and depth of coverage (d10 or higher). Resulting calls were annotated with AnnTools, an exhaustive genome annotation toolkit [Makarov et al., 2011].

Filtering of Common Genetic Variation

Any potential mutation observed as common variation (frequency > 5%) in the dbSNP137 or 1000 Genomes Project Phase 1 was removed for further analyses. Genetic variants mapping to intragenic, intronic, and noncoding exonic regions, with the exception of those variants mapping close to splice sites, were also removed since they are unlikely to be causative. It is worth noting that in the 1000 Genome project, five major populations, including West African, European, American, and East and South Asian, are targeted. Then, a second filter, which consisted of removing common variation (frequency > 5%) present in other public databases, such as the Exome Variant Server of the National Heart, Lung, and Blood Institute (NHLBI) Exome Sequencing Project (http://evs.gs.washington.edu/EVS/) [Exome Variant Server, 2013], exomes generated in house from unaffected members of families with various phenotypes (*n* = 40), and exome data generated in 500 Caucasian control samples that were obtained as VCF files from a large collection of unaffected Caucasian individuals that have been sequenced as part of the ARRA Autism Sequencing Collaboration (AASC) (MH089025, Mark Daly, communicating PI, Joseph D Buxbaum, Bernie Devlin, Richard Gibbs, Gerard Schellenberg, James Sutcliffe, collaborating PI's), was applied to all novel coding genetic mutations found to be present in both siblings. Only variants that we knew for certain that were not pathogenic were included in this second filter. This filter was done last because low frequency
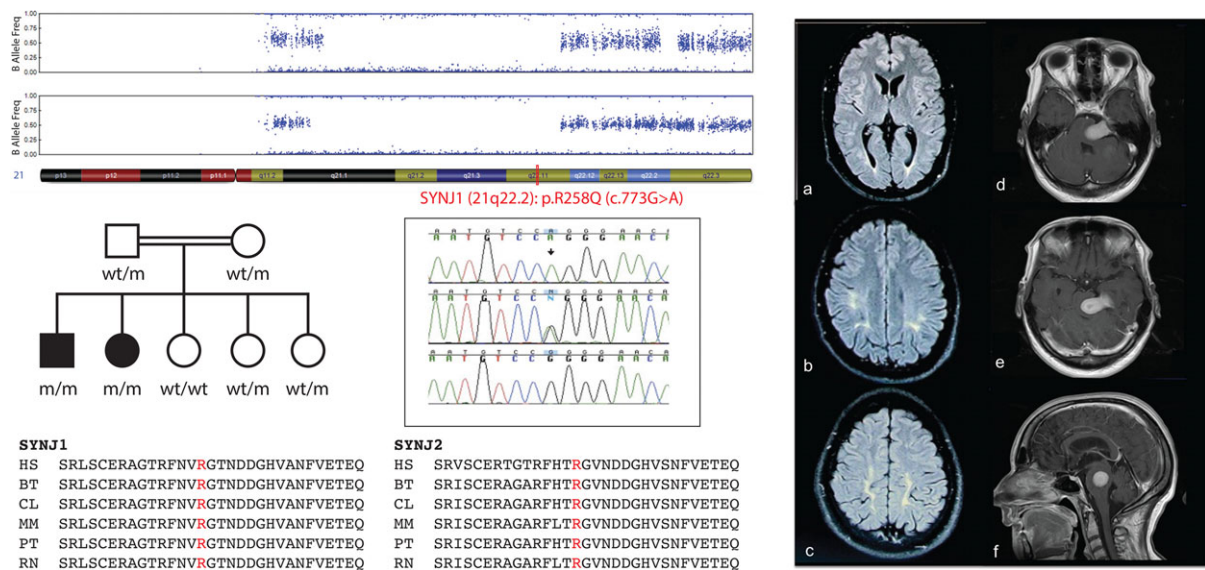
Figure 1. Left side: Upper panel: B allele frequency plots from Genome studio software (Illumina) showing the loss of heterozygosity area (LOH [blank areas]; 21q21.1–22.2) shared by both affected siblings; the location of *SYNJ1* within the disease-associated LOH area is highlighted in red. Middle panel: The pedigree structure of the Iranian family with EOP is shown in the left side while the Sanger chromatograms of the human reference sequence (bottom) as well as both heterozygous (middle) and homozygous (top) mutant sequences are shown in the right side; a black arrow highlights the pathogenic mutation. The p.Arg258Gln mutation is represented as p.R258Q. Bottom panel shows the conservation of R258 amino-acid (highlighted in red) within different orthologs in both SYNJ1 and SYNJ2 proteins. HS: Homo sapiens; BT: Bos Taurus; CL: Canis lupus; MM: Mus musculus; PT: Pan troglodytes; RN: Rattus norvegicus. Right side: Brain FLAIR magnetic resonance images (MRIs) of patient 1 showing bilateral periventricular (a) and subcortical (b and c) white matter hyperintense signals predominantly in parietal-occipital regions. Axial (e and e) and sagittal (f) post-gadolinium brain MR images of patient 2 show an intensely enhancing meningioma with compressing the left pons and lower midbrain. There was no evidence of obstructive hydrocephalus.

Table 1. Homozygous Segments Found only Present in Both Affected Sibling by Homozygosity Mapping Through Genome-Wide SNP Genotyping

CHR	SNP1	SNP2	Position 1 (bp)	Position 2 (bp)	Size (bb)	N° SNP
3	rs9871790	rs2046037	0	2,600,804	2600.8	1039
8	rs11993658	rs16938809	46,886,735	75,062,690	28176	6097
21	**rs171477**	**rs2834280**	**19,150,133**	**35,228,502**	**16078.4**	**4600**

Highlighted in bold is the genomic region turned out to be the disease-associated locus.

genetic alleles could not have been removed, since, for example, low frequency heterozygous alleles may cause a disease when present in the homozygous state.

Prediction of Mutation Pathogenicity

To assist in causative gene identification, the pathogenicity of each novel mutation identified present in both siblings and absent in large number of control individuals was predicted by two computational methods previously evaluated as most efficient [Thusberg et al., 2011]: MutPred (http://mutpred.mutdb.org/) and SNPs&GO (http://snps-and-go.biocomp.unibo.it/snps-and-go/). All sequence variant descriptions were also examined using the Mutalyzer program (http://www.LOVD.nl/mutalyzer/). The HomoloGene database from NCBI web site was also used to examine the conservation of both disease-segregating mutations in different species (http://www.ncbi.nlm.nih.gov/homologene). Clustalw2 was also used to align Synaptojanin 1 with other human proteins containing Sac1 domains (http://www.ebi.ac.uk/Tools/msa/clustalw2/).

Gene Screening Analyses

Genomic primers for PCR amplifications were designed using a primer design public website (http://ihg.gsf.de/ihg/ExonPrimer.html). Primers were used to amplify exon 7 of *MCM4*, exon 3 of *SPATA31A1* (previous symbol, *FAM75A1*), and all coding exons of *SYNJ1* (primer sequences available upon request). PCR amplifications were performed as previously described [Karkheiran et al., 2012]. All purified PCR products were then sequenced in both forward and reverse directions with Applied Biosystems BigDye terminator v3.1 sequencing chemistry as per the manufacturer's instructions. The resulting sequencing reactions were resolved on an ABI3130 genetic analyzer (Applied Biosystems, Foster City, CA) and analyzed using Sequencer 5.0 software (Gene Codes Corporation, Ann Arbor, MI).

Mutagenesis and Protein Expression and Purification

Direct mutagenesis was done using the QuikChange Lightning Site-Directed Mutagenesis kit (Stratagene, Agilent Technologies Inc.), both pcDNA3-FLAG-human-Synaptojanin 1–145 and pEGFPC1-FLAG-human-Synaptojanin 1–145 (Addgene: http://www.addgene.org/22291/ and http://www.addgene.org/22293/, respectively) and corresponding primers (Primer sequences available upon request). Plasmids were purified using the Plasmid Purification Maxi kit for high-copy plasmids. The tagged human SYNJ1 wild-type and mutants were transfected into HEK293T cells using Lipofectamine 2000 (Invitrogen, Life Technologies, Grand Island, NY) and purified by immunoprecipitation on anti-FLAG M2 bead. Protein concentration of affinity purified SYNJ1 was determined by loading BSA protein standards alongside purified SYNJ1 and

Table 2. Homozygous SNPs Identified in Both Affected Siblings after Performing Whole-Exome Sequencing Followed by Adequate Filtering

Chr	Position (bp)	Gene	MIM (#)	Nucleotide change	Protein change	Pathogenicity's prediction[a]	Control data	Brain expression	Function/Associated disease
8	**48,877,146**	**MCM4**	**602638**	**c.706A>G**	**p.Thr236Ala**	**0.493/Neutral**	**0/376**	**Cerebral cortex, cerebellum, hippocampus**	**Adrenal insufficiency, short stature, NK cell deficiency, and FGD**
9	39,357,781	SPATA31A1[b]	N.A	c.274C>G	p.Gln92Glu	0.213/Neutral	Not examined	No Information	Unknown
21	**34,067,416**	**SYNJ1**	**604297**	**c.773G>A**	**p.Arg258gln**	**0.877/Disease**	**0/376**	**Cerebral cortex, cerebellum, hippocampus**	**Synaptic vesicle recycling**

Chromosome position, affected gene, nucleotide and protein changes, expression data, as well as function or associated disease are shown for each SNP identified. The nt numbering reflects cDNA with +1 as the A of the ATG initiation codon in the reference sequence (www.hgvs.org/mutnomen). The initiation codon is codon 1. Highlighted in bold are the disease-segregating mutations also found present in previously shown disease-associated loci (Table 1).
[a]Predictions are based on MutPred and SNPs&GO computational methods.
[b]Previous symbol, FAM75A1.
NK, natural killer; FGD, Familial glucocorticoid deficiency P.Gln92Glu mutation did not segregate with disease.

performing SDS-PAGE followed by coomassie blue staining (Invitrogen, Life Technologies). Western Blot was performed using anti-FLAG M2 antibody (Sigma–Aldrich, St. Louis, MO) to show equal amounts of affinity purified wild-type and mutant SYNJ1. Anti β-Actin antibody (8H10D10) (Cell Signaling Technology, Danvers, MA) was used as loading control.

Malachite Green-Based Phosphatase Assay

Enzymatic activity of wild-type and mutants SYNJ1 was measured by malachite-green based assays. The final assay mixture (25 μl) contained either 1 μg of PI(4,5)P$_2$, 10 μg of PI3P or PI4P, and 250 ng enzyme with 1 μg substrate or 500 ng enzyme with 10 μg substrate. Reactions were incubated for 30 min at 37°C and the supernatants were added to 80 μl of malachite green solution (Echelon Biosciences Inc., Salt Lake City, UT) and allowed to incubate for 5 min at 37°C, and then at room temperature for another 5 min. The absorbance was measured by plate reader at a wavelength of 620 nm and normalized to the wild-type value.

Statistical Analyses

All the data are expressed as the mean ± SEM. Graphics represent means and SEM of at least nine independent experiments. The statistical differences between wild-type and both mutants synaptojanin 1 were determined by a nonparametric test like Mann–Whitney U test, in which P values of $P \leq 0.001$ were considered highly significant (***).

Reporting Pathogenic Genetic Variants

The genetic variant identified in this study as pathogenic is now included in an existing locus-specific database at http://databases.lovd.nl/shared/genes/SYNJ1.

Results

We report two affected siblings suffering from EOP and generalized seizures. The main clinical features of both patients are described below.

Patients' Clinical Details

Patient I

This 29-year-old man was born to consanguineous parents. At the age of 3 years, he developed generalized seizures, which responded to phenobarbital. At the age of 20, he developed a right hand tremor and progressive bradykinesia. Within 2 years, he developed severe bradykinesia, bilateral hand (R>L) and chin tremor, apraxia of eyelid opening (ALO), and dysarthria. He was treated with trihexyphenidyl and L-dopa/carbidopa with improvement in both tremor and bradykinesia but soon developed L-dopa-induced dyskinesias at very low doses (50 mg). Because of severity of dyskinesia, L-dopa was stopped and he was treated with the dopamine agonist bromocriptine up to 15 mg/day with modest improvement of all Parkinsonian symptoms and a reduction in dyskinesia. There was no sign of cognitive impairment. He continued taking phenobarbital for over 20 years with acceptable seizure control until 3 years ago; he now only has one to two seizures per year.

On physical examination at the age of 29, he had generalized bradykinesia with bilateral limb rigidity, right side predominant resting tremor, chin tremor, and inability to open his eyelids spontaneously. He had jerky saccades and saccadic pursuits. His speech was unintelligible due to severe hypophonia and his gait was shuffling with postural instability. Off medication Unified Parkinson Disease Rating Scale part III (UPDRS-III) score was 38 (maximum score = 56) with most scores related to bradykinesia and rigidity. Muscle strength, deep tendon reflexes, cerebellar, and sensory functions were all normal. Administration of 25 mg/day of L-dopa completely alleviated the ALO and improved bradykinesia, rigidity, oculomotor abnormalities, and shuffling gait. One hour after medication administration, his gait was normal, his speech became more intelligible, but postural instability was unchanged. Wearing off started to appear 2 hr after drug administration (The UPDRS-III scores were 28 and 18 at 30 min and 1 hr respectively after taking levodopa, the latter being mostly due to rest tremor). With doses greater than 25 mg of levodopa, in addition to dyskinesias, the patient became euphoric and talkative. There was no evidence of hyposmia, urinary urgency, incontinence, erectile dysfunction, constipation, or orthostatic hypotension. During the "on" period, cognitive functioning was intact with moderate bradyphrenia. Brain MRI showed mild cortical atrophy and bilateral symmetric T2 hyperintensities in the white matter, mostly posteriorly (Figure 1a–c).

Patient II

This 39-year-old woman had a febrile convulsion in infancy followed by unprovoked generalized tonic–clonic seizures for which she was treated with phenobarbital. Developmental milestones were normal. In her early twenties, she developed a right hand tremor, followed by bradykinesia, severe jaw tremor, and eyelid twitching. The disease progression was similar to that of her brother. She could walk unassisted until the age of 32 years, but subsequently required assistance. She had severe dyskinesia with small doses of levodopa (25 mg) and nonergot dopamine agonists, and only tolerated anticholinergics and bromocriptine, which gave her good tremor control and moderate improvement in bradykinesia. Cognitive function was grossly normal. Brain MRI performed at 37 years old showed a large foramen magnum meningioma (Figure 1d–f). After surgery to remove this tumor, the patient lost her ability to walk and became bedbound. During her last visit, at the age of 39, she was anarthric and in fixed "quadriplegia in flexion" posture, but she correctly responded to "open and close your eyes" and "make a sound" commands. Mass lesions compressing the brainstem may cause Parkinsonism; however, the *SYNJ1* mutation, shared with her brother, and not this lesion, are likely to be responsible for our patient's clinical syndrome. The absence of localizing corticospinal signs and the lack of surrounding edema seen on MRI indicate that the tumor grew extremely slowly, displacing the brainstem without causing significant neuronal dysfunction. The patient's seizures could not be attributed to this tumor. Although not illustrated here, other views of the brain MRI clearly show that there was no evidence of obstruction of cerebrospinal fluid flow through the aqueduct and the lateral ventricles were of normal size. In addition, the features of Parkinsonism seen here are not observed in ventricular obstruction.

Molecular Analyses

All available family members ($n = 7$) were subject to genome-wide SNP genotyped analyses and HM, which revealed three potential disease-associated loci. These loci, only shared by the two affected siblings, were located at chromosomes 3, 8, and 21 (Table 1). No shared region of homozygosity or copy number variation was identified within the known PD loci. The WES performed in the two affected siblings captured 95.18% and 95.88% of the target exome at 20-fold coverage or higher for patients I and II, respectively. This leads us to the high-quality identification of 61,286 SNVs and 9,836 indels for Patient I and 67,337 SNVs and 13,061 indels for Patient II. All known PD genes were well covered by our WES approaches and excluded. After an adequate filtering (see methods), 832 nonsynonymous, 11 nonsense, and 459 synonymous genetic variants were identified for Patient I, whereas 982 nonsynonymous, 10 nonsense, and 463 synonymous genetic variants were identified for Patient II. None of the nonsense genetic variants were present in both patients and only 223 nonsynonymous genetic variants (187 heterozygous and 36 homozygous) were common to both affected siblings. Further investigation of the 223 novel genetic variants in the dbSNP137, in other public databases, and exomes generated in house (see *Methods*) left us with only three novel genetic variants present in both siblings (Table 2). Two of these, c.706A>G (p.Thr236Ala) within minichromosome maintenance complex component 4 (*MCM4*; 8q11.2) and c.773G>A (p.Arg258Gln) within synaptojanin 1 (*SYNJ1;* 21q22.2), were located in genomic regions previously found associated with disease through homozygosity mapping (Tables 1 and 2). The genotyping area harboring the third variant (*SPATA31A1* locus) was additionally inspected, but only a small homozygous area of 91 kb also shared by unaffected individual was

identified. As expected, subsequent sequencing of this variant in all family members revealed that it does not segregate with disease. Both variants located within the disease-associated loci were subsequently validated through Sanger sequencing and examined in the remaining family members: both mutations were present in the homozygous state in both affected siblings while both parents were heterozygous mutation carriers and unaffected members were either homozygous carriers for the wild-type allele or heterozygous mutation carriers, clearly consistent with a disease-segregation status. Further testing of both mutations in 376 control chromosomes (184 Caucasians and 192 Iranians) failed to identify any additional mutation carrier. However, it is very unlikely that the phenotype observed in our patients is due to the p.Thr236Ala mutation in *MCM4*, which is essential for the initiation of eukaryotic genome replication, since it was predicted to be noncausative and *MCM4* mutations have recently been associated with clinical features, such as autosomal recessive adrenal insufficiency, short stature, natural killer cell deficiency, and familial glucocorticoid deficiency [Casey et al., 2013; Hughes et al., 2012; Yamaguchi et al., 2013], not present in our patients (Table 2). Moreover, none of the patients already described with pathogenic *MCM4* mutations showed signs of Parkinsonism; and although none of the *MCM4* mutations identified, including the one described here, lie within a functional domain, they all seem to be located throughout the protein, ruling out the possibility that *MCM4*-associated phenotypes are determined by the localization of the mutation within the protein. By contrast, the p.Arg258Gln mutation in *SYNJ1,* a highly brain enriched polyphosphoinositide phoshatase involved in synaptic vesicle recycling [Cremona et al., 1999; McPherson et al., 1996], was predicted to be pathogenic. This amino-acid change results from a G>A mutation at position 258 for transcripts 1 (NM_003895.3) and 2 (NM_203446.2) and 219 for transcripts 3 (NM_001160302.1) and 4 (NM_001160306.1). *SYNJ1* comprises two inositol phosphatase domains arranged in tandem— an N-terminal Sac1 inositol phosphatase domain and a central inositol 5-phosphatase domain—followed by a COOH-terminal proline-rich region that interacts with a variety of protein factors implicated in signaling, endocytosis, and actin nucleation [McPherson et al., 1996; Slepnev and De Camilli, 2000]. The Sac 1 domain dephosphorylates PI3P, PI4P, and PI(3,5)P$_2$ [Guo et al., 1999], whereas the preferred substrates of the 5-phosphatase domain are PI(4,5)P$_2$ and PI(3,4,5)P$_3$ [Cremona et al., 1999]. The p.R219/258 amino-acid is localized in the Sac1 domain and is highly conserved among 18 different orthologs and in the SYNJ2 protein (NM_003889), which has a similar domain structure but more widespread tissue distribution than SYNJ1 [Nemoto et al., 1997] (Figure 1); it is also conserved among three other human proteins containing Sac1 domains, including SACM1L (SAC1, NM_014016.3), INPP5F (SAC2, NM_014937), and FIG4 (SAC3, NM_014845) proteins (data not shown). Taking into account all public SNPs databases, exomes generated in house, and DNA control samples testing by direct Sanger sequencing, p.Arg258Gln was absent in over 10,000 control chromosomes, likely supporting its pathogenicity.

Although 20 DNA samples of affected individuals with complex EOP were additionally tested for the entire coding region of *SYNJ1*, we failed to identify any other mutation carrier.

We thus tested whether the p.Arg258Gln (p.Arg219Gln) mutation impairs the phosphoinositide phosphatase activity of the Sac1 domain. The c.1149T>A/c.1264T>A (p.Cys383Ser/p.Cys422Ser) mutation in the Sac1 domain of human SYNJ1 domain was used as a control, based on previous work showing that p.Cys383Ser impairs the Sac1-like phosphatase activity toward PI3P and PI4P [Mani et al., 2007]. This analysis showed that while p.Cys383Ser (p.Cys422Ser) and p.Arg219Gln (p.Arg258Gln) mutations did not affect in a
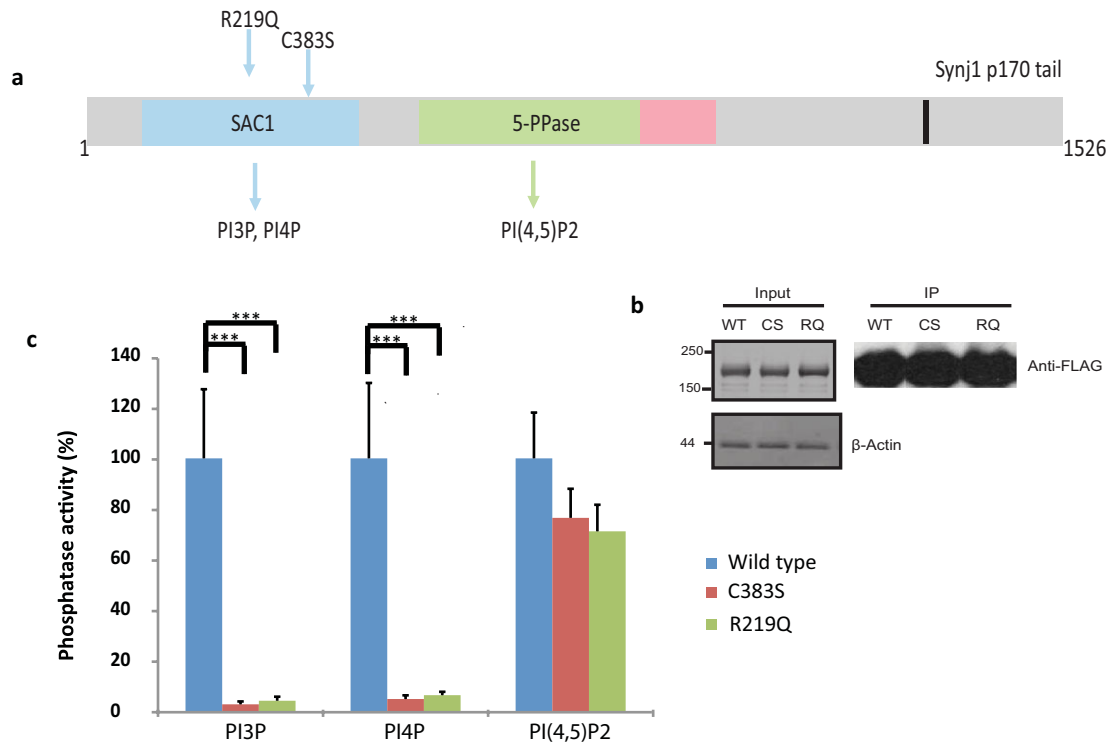
Figure 2. **A:** Domain organization of SYNJ1–145 (3) and SYNJ1–170 (4) isoforms [Haffner et al., 1997; Perera et al., 2006]. SYNJ1–145 is highly expressed in the nervous system, specifically in mature brain and synapses, while the alternatively spliced isoform SYNJ1–170, which has a longer C-terminal, is ubiquitously expressed but at lower levels. The domain organization was drawn based on published reports and SMART predictions (http://smart.embl-heidelberg.de/) [Guo et al., 1999; Jha et al., 2004] and includes the two polyphosphoinositide phosphatase regions and the C-terminal region, which is responsible for protein–protein interactions. The extended C-terminal tail of SYNJ1–170 contains binding sites for proteins of the endocytic machinery. Both p.Arg219Gln (R219Q or R258Q) and p.Cys383Ser (C383S or C422S) mutations lying in the Sac1-like region are shown. **B:** Anti-Flag Western-blot showing equal amounts of affinity purified Flag-tagged wild-type and mutant SYNJ1. **C:** Wild-type and mutants SYNJ1 were expressed in HEK 293T cells and purified by immunoprecipitation. The enzymatic activity was measured by malachite-green based assays. Error bars are SEM. Graphics represent means and SEM of at least nine independent experiments. (***) indicates P values of $P \leq 0.001$.

significant way the phosphatase activity against PI(4,5)P$_2$, which is known to be accounted by the 5-phosphatase domain of SYNJ1, they drastically inhibited the phosphatase activity against PI3P and PI4P (Figure 2c), as expected for mutations that impair the Sac1-like phosphatase activity of this enzyme [Guo et al., 1999].

Discussion

We report on a consanguineous family with autosomal recessive EOP with generalized seizures. Two siblings developed seizures in early childhood, followed by resting hand tremor and bradykinesia in their early 20's, and progressing to chin tremor and ALO. HM, WES, and gene screening analyses led us to the identification of three disease-associated loci and two disease-segregating genetic variants (Tables 1 and 2). Both disease-segregating variants, p.Thr236Ala and p.Arg258Gln, were absent in controls, including some of Iranian ancestry. Although the Iranian control population tested here was not large, given the high rate of consanguinity extant in the Iranian population [Akrami and Osati, 2007], the prevalence of a rare private allele in this population is much higher than the generally expected [Bittles and Black, 2010]. Moreover, our follow up investigations in the most likely disease-causing mutation and the only one predicted to be pathogenic, provided additional evidences to support the p.Arg258Cys mutation as the disease-causing mutation. Previous studies demonstrated that the synaptic function of SYNJ1

depends on its intact dual phosphatase activity [Mani et al., 2007]. Here, we showed that the disease-linked mutation almost entirely eliminated both 3-phosphatase and 4-phosphatase activities (Figure 2c), which also suggests that the patients carrying this mutation may have increased levels of SYNJ1 substrates. The inhibition of the Sac-1 activity is expected to impair synaptic vesicle endocytosis and reavailability in nerve terminals, as suggested by previous reports and studies done in mice [Cremona et al., 1999; Mani et al., 2007].

The identification of a *SYNJ1* mutation linked to Parkisonism is interesting because this lipid metabolizing enzyme is a key regulator of phosphoinositide metabolism in the nervous system and has been shown to regulate key synaptic processes, such as the recycling of synaptic vesicles, the internalization of AMPA receptors, as well as actin dynamics [Frere et al., 2012; Gad et al., 2000; Gong and De Camilli, 2008; Harris et al., 2000; Verstreken et al., 2003]. Although *SYNJ1* mutations have not been previously associated with a human neurological disease, the overexpression of this protein in Down syndrome mouse models causes a deficiency of PI(4,5)P$_2$ as well as learning deficits [Voronov et al., 2008], whereas Synj1 haploinsufficiency is protective against the synaptotoxic action of beta-amyloid in vitro and in mouse models of Alzheimer disease [Berman et al., 2008; McIntire et al., 2012]. Additionally, *Synj1* knockout mice fail to thrive and rapidly develop severe neurological manifestations including severe weakness, ataxia, spontaneous epileptic seizures, and poor motor coordination [Cremona et al., 1999]; and loss of SYNJ function in *Caenorhabditis elegans*, zebrafish, and *drosophila*

results in severe nervous system defects mutants, such as abnormal balance, posture, and locomotion [Harris et al., 2000; Minagawa et al., 2001; Stefan et al., 2002; Van Epps et al., 2004; Verstreken et al., 2003].

There is mounting evidence that synaptic vesicle trafficking pathways are implicated in neurodegeneration [Esposito et al., 2012]. Alpha-synuclein has been implicated in synaptic vesicle exocytosis and in synaptic vesicle recycling [Burre et al., 2010; Nemani et al., 2010]. *LRRK2* mutations also cause a defect in synaptic vesicle endocytosis, which can be rescued by co-expression of Rab5b [Heo et al., 2010]. LRRK2 has also been identified as regulator of endophilin-A [Matta et al., 2012], which is a major binding partner of SYNJ1 and interacts and participates with Parkin in the ubiquitination of proteins within synaptic endophilin-A complexes [Trempe et al., 2009]. And lastly, disruption of the SYNJ1/endophilin interaction by Cdk5, which phosphorylates parkin [Rubio de laTorre et al., 2009; Yamamoto et al., 2005] and SYNJ1 [Tan et al., 2003], has been suggested to be important for synaptic vesicles recycling [Lee et al., 2004].

These findings add further support to the evidence that many Parkinsonism-associated proteins, including alpha-synuclein, parkin, dardarin (LRRK2), auxilin, and now also SYNJ1, act as important regulators of synaptic vesicle trafficking pathways at synapses. All together they foster the hypothesis that aberrant functions of proteins implicated in the SV recycling may be responsible for at least part of the neuronal cell loss seen in Parkinson disease and other neurodegenerative diseases.

In conclusion, our data support the disease-segregating p.Arg258Gln (p.Arg219Gln) mutation, which is absent in over 10,000 control chromosomes and impairs the Sac1-like domain activity, as the genetic cause responsible for autosomal recessive Parkinsonism with generalized seizures in our patients. Although further studies are warranted to gain insights into the mechanisms by which dysfunction of phosphoinositide phosphatases, such as synaptojanin 1, results in neurological dysfunction and likely cell death, our current finding opens a new avenue of investigation in the field of Parkinson research, adds further evidence that defects in membrane trafficking at the synapse may be key factors in the development of both Parkinson disease and Parkinsonism, and suggests phosphoinositide metabolism as a novel therapeutic target for Parkinsonism.

Acknowledgments

References

Akrami SM, Osati Z. 2007. Is consanguineous marriage religiously encouraged? Islamic and Iranian considerations. J Biosoc Sci 39(2):313–316.

Berman DE, Dall'Armi C, Voronov SV, McIntire LB, Zhang H, Moore AZ, Staniszewski A, Arancio O, Kim TW, Di Paolo G. 2008. Oligomeric amyloid-beta peptide disrupts phosphatidylinositol-4,5-bisphosphate metabolism. Nat Neurosci 11(5):547–554.

Bittles AH, Black ML. 2010. Evolution in health and medicine Sackler colloquium: consanguinity, human evolution, and complex diseases. Proc Natl Acad Sci USA 107 Suppl 1:1779–1786.

Burre J, Sharma M, Tsetsenis T, Buchman V, Etherton MR, Sudhof TC. 2010. Alpha-synuclein promotes SNARE-complex assembly in vivo and in vitro. Science 329(5999):1663–1667.

Camargos S, Scholz S, Simon-Sanchez J, Paisan-Ruiz C, Lewis P, Hernandez D, Ding J, Gibbs JR, Cookson MR, Bras J, Guerreiro R, Oliveira CR, et al. 2008. DYT16, a novel young-onset dystonia-Parkinsonism disorder: identification of a segregating mutation in the stress-response protein PRKRA. Lancet Neurol 7(3):207–215.

Casey JP, Nobbs M, McGettigan P, Lynch S, Ennis S. 2013. Recessive mutations in MCM4/PRKDC cause a novel syndrome involving a primary immunodeficiency and a disorder of DNA repair. J Med Genet 49(4):242–245.

Cremona O, Di Paolo G, Wenk MR, Luthi A, Kim WT, Takei K, Daniell L, Nemoto Y, Shears SB, Flavell RA, McCormick DA, De Camilli P. 1999. Essential role of phosphoinositide metabolism in synaptic vesicle recycling. Cell 99(2):179–188.

DePristo MA, Banks E, Poplin R, Garimella KV, Maguire JR, Hartl C, Philippakis AA, del Angel G, Rivas MA, Hanna M, McKenna, Fennell TJ, et al. 2011. A framework for variation discovery and genotyping using next-generation DNA sequencing data. Nat Genet 43(5):491–498.

Dittman J, Ryan TA. 2009. Molecular circuitry of endocytosis at nerve terminals. Annu Rev Cell Dev Biol 25:133–160.

Edvardson S, Cinnamon Y, Ta-Shma A, Shaag A, Yim YI, Zenvirt S, Jalas C, Lesage S, Brice A, Taraboulos A, Kaestner KH, Greene LE, Elpeleg O. 2012. A deleterious mutation in DNAJC6 encoding the neuronal-specific clathrin-uncoating co-chaperone auxilin, is associated with juvenile Parkinsonism. PLoS One 7(5):e36458.

Esposito G, Ana Clara F, Verstreken P. 2012. Synaptic vesicle trafficking and Parkinson's disease. Dev Neurobiol 72(1):134–144.

Exome Variant Server. 2013. NHLBI Exome Sequencing Project (ESP), Seattle, WA. Accessed May, 2013, at: http://evs.gs.washington.edu/EVS/.

Frere SG, Chang-Ileto B, Di Paolo G. 2012. Role of phosphoinositides at the neuronal synapse. Subcell Biochem 59:131–175.

Gad H, Ringstad N, Low P, Kjaerulff O, Gustafsson J, Wenk M, Di Paolo G, Nemoto Y, Crun J, Ellisman MH, De Camilli P, Shupliakov O, Brodin L. 2000. Fission and uncoating of synaptic clathrin-coated vesicles are perturbed by disruption of interactions with the SH3 domain of endophilin. Neuron 27(2):301–312.

Gong LW, De Camilli P. 2008. Regulation of postsynaptic AMPA responses by synaptojanin 1. Proc Natl Acad Sci USA 105(45):17561–17566.

Guo S, Stolz LE, Lemrow SM, York JD. 1999. SAC1-like domains of yeast SAC1, INP52, and INP53 and of human synaptojanin encode polyphosphoinositide phosphatases. J Biol Chem 274(19):12990–12995.

Haffner C, Takei K, Chen H, Ringstad N, Hudson A, Butler MH, Salcini AE, Di Fiore PP, De Camilli P. 1997. Synaptojanin 1: localization on coated endocytic intermediates in nerve terminals and interaction of its 170 kDa isoform with Eps15. FEBS Lett 419(2–3):175–180.

Hardy J, Lewis P, Revesz T, Lees A, Paisan-Ruiz C. 2009. The genetics of Parkinson's syndromes: a critical review. Curr Opin Genet Dev 19(3):254–265.

Harris TW, Hartwieg E, Horvitz HR, Jorgensen EM. 2000. Mutations in synaptojanin disrupt synaptic vesicle recycling. J Cell Biol 150(3):589–600.

Heo HY, Kim KS, Seol W. 2010. Coordinate regulation of neurite outgrowth by LRRK2 and its interactor, Rab5. Exp Neurobiol 19(2):97–105.

Hughes CR, Guasti L, Meimaridou E, Chuang CH, Schimenti JC, King PJ, Costigan C, Clark AJ, Metherell LA. 2012. MCM4 mutation causes adrenal failure, short stature, and natural killer cell deficiency in humans. J Clin Invest 122(3):814–820.

Jankovic J. 2008. Parkinson's disease: clinical features and diagnosis. J Neurol Neurosurg Psychiatry 79(4):368–376.

Jha A, Agostinelli NR, Mishra SK, Keyel PA, Hawryluk MJ, Traub LM. 2004. A novel AP-2 adaptor interaction motif initially identified in the long-splice isoform of synaptojanin 1, SJ170. J Biol Chem 279(3):2281–2290.

Karkheiran S, Krebs CE, Makarov V, Nilipour Y, Hubert B, Darvish H, Frucht S, Shahidi GA, Buxbaum JD, Paisan-Ruiz C. 2012. Identification of COL6A2 mutations in progressive myoclonus epilepsy syndrome. Hum Genet 132(3):275–283.

Koroglu C, Baysal L, Cetinkaya M, Karasoy H, Tolun A. 2013. DNAJC6 is responsible for juvenile Parkinsonism with phenotypic variability. Parkinsonism Relat Disord 19(3):320–324.

Krebs CE, Paisan-Ruiz C. 2012. The use of next-generation sequencing in movement disorders. Front Genet 3:75.

Kurian MA, Zhen J, Cheng SY, Li Y, Mordekar SR, Jardine P, Morgan NV, Meyer E, Tee L, Pasha S, Wassmer E, Heales SJ, et al. 2009. Homozygous loss-of-function mutations in the gene encoding the dopamine transporter are associated with infantile Parkinsonism-dystonia. J Clin Invest 119(6):1595–1603.

Lee SY, Wenk MR, Kim Y, Nairn AC, De Camilli P. 2004. Regulation of synaptojanin 1 by cyclin-dependent kinase 5 at synapses. Proc Natl Acad Sci USA 101(2):546–551.

Li H, Durbin R. 2009. Fast and accurate short read alignment with Burrows–Wheeler transform. Bioinformatics 25(14):1754–1760.

Makarov V, O'Grady T, Cai G, Lihm J, Buxbaum JD, Yoon S. 2011. AnnTools: a comprehensive and versatile annotation toolkit for genomic variants. Bioinformatics 28(5):724–725.

Mani M, Lee SY, Lucast L, Cremona O, Di Paolo G, De Camilli P, Ryan TA. 2007. The dual phosphatase activity of synaptojanin1 is required for both efficient synaptic vesicle endocytosis and reavailability at nerve terminals. Neuron 56(6): 1004–1018.

Martin I, Dawson VL, Dawson TM. 2011. Recent advances in the genetics of Parkinson's disease. Annu Rev Genomics Hum Genet 12:301–325.

Matta S, Van Kolen K, da Cunha R, van den Bogaart G, Mandemakers W, Miskiewicz K, De Bock PJ, Morais VA, Vilain S, Haddad D, Delbroek L, Swerts J, et al. 2012. LRRK2 controls an EndoA phosphorylation cycle in synaptic endocytosis. Neuron 75(6):1008–1021.

McIntire LB, Berman DE, Myaeng J, Staniszewski A, Arancio O, Di Paolo G, Kim TW. 2012. Reduction of synaptojanin 1 ameliorates synaptic and behavioral impairments in a mouse model of Alzheimer's disease. J Neurosci 32(44):15271–15276.

McPherson PS, Garcia EP, Slepnev VI, David C, Zhang X, Grabs D, Sossin WS, Bauerfeind R, Nemoto Y, De Camilli P. 1996. A presynaptic inositol-5-phosphatase. Nature 379(6563):353–357.

Minagawa T, Ijuin T, Mochizuki Y, Takenawa T. 2001. Identification and characterization of a sac domain-containing phosphoinositide 5-phosphatase. J Biol Chem 276(25):22011–22015.

Nemani VM, Lu W, Berge V, Nakamura K, Onoa B, Lee MK, Chaudhry FA, Nicoll RA, Edwards RH. 2010. Increased expression of alpha-synuclein reduces neurotransmitter release by inhibiting synaptic vesicle reclustering after endocytosis. Neuron 65(1):66–79.

Nemoto Y, Arribas M, Haffner C, DeCamilli P. 1997. Synaptojanin 2, a novel synaptojanin isoform with a distinct targeting domain and expression pattern. J Biol Chem 272(49):30817–30821.

Paisan-Ruiz C, Guevara R, Federoff M, Hanagasi H, Sina F, Elahi E, Schneider SA, Schwingenschuh P, Bajaj N, Emre M, Singleton AB, Hardy J, et al. 2010. Early-onset L-dopa-responsive Parkinsonism with pyramidal signs due to ATP13A2, PLA2G6, FBXO7 and spatacsin mutations. Mov Disord 25(12):1791–1800.

Perera RM, Zoncu R, Lucast L, De Camilli P, Toomre D. 2006. Two synaptojanin 1 isoforms are recruited to clathrin-coated pits at different stages. Proc Natl Acad Sci USA 103(51):19332–19337.

Purcell S, Neale B, Todd-Brown K, Thomas L, Ferreira MA, Bender D, Maller J, Sklar P, de Bakker PI, Daly MJ, Sham PC. 2007. PLINK: a tool set for whole-genome association and population-based linkage analyses. Am J Hum Genet 81(3): 559–575.

Rubio de la Torre E, Luzon-Toro B, Forte-Lago I, Minguez-Castellanos A, Ferrer I, Hilfiker S. 2009. Combined kinase inhibition modulates parkin inactivation. Hum Mol Genet 18(5):809–823.

Singleton AB. 2011. Exome sequencing: a transformative technology. Lancet Neurol 10(10):942–946.

Slepnev VI, De Camilli P. 2000. Accessory factors in clathrin-dependent synaptic vesicle endocytosis. Nat Rev Neurosci 1(3):161–172.

Stefan CJ, Audhya A, Emr SD. 2002. The yeast synaptojanin-like proteins control the cellular distribution of phosphatidylinositol (4,5)-bisphosphate. Mol Biol Cell 13(2):542–557.

Tan TC, Valova VA, Malladi CS, Graham ME, Berven LA, Jupp OJ, Hansra G, McClure SJ, Sarcevic B, Boadle RA, Larsen MR, Cousin MA, Robinson PJ. 2003. Cdk5 is essential for synaptic vesicle endocytosis. Nat Cell Biol 5(8):701–710.

Thusberg J, Olatubosun A, Vihinen M. 2011. Performance of mutation pathogenicity prediction methods on missense variants. Hum Mutat 32(4):358–368.

Trempe JF, Chen CX, Grenier K, Camacho EM, Kozlov G, McPherson PS, Gehring K, Fon EA. 2009. SH3 domains from a subset of BAR proteins define a Ubl-binding domain and implicate parkin in synaptic ubiquitination. Mol Cell 36(6): 1034–1047.

Van Epps HA, Hayashi M, Lucast L, Stearns GW, Hurley JB, De Camilli P, Brockerhoff SE. 2004. The zebrafish nrc mutant reveals a role for the polyphosphoinositide phosphatase synaptojanin 1 in cone photoreceptor ribbon anchoring. J Neurosci 24(40):8641–8650.

Verstreken P, Koh TW, Schulze KL, Zhai RG, Hiesinger PR, Zhou Y, Mehta SQ, Cao Y, Roos J, Bellen HJ. 2003. Synaptojanin is recruited by endophilin to promote synaptic vesicle uncoating. Neuron 40(4):733–748.

Voronov SV, Frere SG, Giovedi S, Pollina EA, Borel C, Zhang H, Schmidt C, Akeson EC, Wenk MR, Cimasoni L, Arancio O, Davisson MT, et al. 2008. Synaptojanin 1-linked phosphoinositide dyshomeostasis and cognitive deficits in mouse models of Down's syndrome. Proc Natl Acad Sci USA 105(27):9415–9420.

Yamaguchi R, Kato F, Hasegawa T, Katsumata N, Fukami M, Matsui T, Nagasaki K, Ogata T. 2013. A novel homozygous mutation of the nicotinamide nucleotide transhydrogenase gene in a Japanese patient with familial glucocorticoid deficiency. Endocr J. Doi: 10.1507/endocrj. EJ13-0024. [Epub ahead of print.]

Yamamoto A, Friedlein A, Imai Y, Takahashi R, Kahle PJ, Haass C. 2005. Parkin phosphorylation and modulation of its E3 ubiquitin ligase activity. J Biol Chem 280(5):3390–3399.